[O III] imaging surveys would be useful.

Whilst there are differences between the abundances of the two Sagittarius PN – He 2-436 has a low N abundance – the values generally bracket the abundances for the Fornax PN. The O abundances of He 2-436 and Wray 16-423 differ by only 0.08 dex and the mean of both is 12+Log(O/H)=8.35. The value for the Fornax PN is 8.5 (Danziger et al., 1978). Whilst the O/H abundances of these three PN are lower (by ∼0.4 dex) than the average for Galactic PN, they are not as low as that of Compact Blue Galaxies ([O/H]∼8.1, e.g. Pagel & Edmunds, 1981), indicating that the PN belong to later generations of star formation. The PN can therefore be regarded as arising in an intermediate-age population and provide a unique diagnostic of the abundances of the light elements, which are difficult to determine from stellar spectra. Mateo et al., (1995) derived an Fe/H abundance of 8% compared to solar for the Sagittarius dwarf, suggesting that [O/Fe] (log O/Fe) is +0.6. Incidentally, the errors on the oxygen abundance are much lower than the errors on the Fe abundance, the latter measured from the integrated stellar population. The [O/Fe] value in the Sagittarius dwarf is higher than for the Galaxy and the Magellanic Clouds (+0.45 and –0.3 respectively, Richer & McCall, 1995), consistent with the galactic evolution models of Matteucci & Brocato (1990).

Although only three planetary nebulae have so far been confirmed in dwarf spheroidal galaxies, they clearly have a pivotal role to play in understanding the star-formation history in these dwarf galaxy systems.

References

Acker, A., Ochsenbein, F., Stenholm, B., Tylenda, R., Marcout, J., Schohn, C., 1992, *Strasbourg - ESO Catalogue of Galactic Planetary Nebulae,* ESO.

Danziger, I. J., Dopita, M. A., Hawarden, T. G., Webster, B. L., 1978, *ApJ*, **220**, 458.

Edmunds. M. G., Pagel, B. E. J., 1981, *ARAA*, **19**, 77.

Ibata, R. A., Gilmore, G., Irwin, M. J., 1994, *Nature*, **370**, 194.

Ibata, R. A., Gilmore, G., Irwin, M. J., 1995, *MNRAS*, **277**, 781.

Jacoby, G. H., Fullton, L., Morse, J., Phillips, M., 1996, paper presented at the IAU Symposium No. 180 on Planetary Nebulae, Groningen.

Mateo, M., Udalski, A., Szymanski, M., Kaluzny, J., Kubiak, M., Krzeminski, W., 1995, *AJ*, **109**, 588.

Mateo, M., Mirabel, N., Udalski, A., Szymanski, M., Kaluzny, J., Kubiak, M., Krzeminski, W., Stanek, K. Z., 1996, *ApJ*, **458**, L43.

Matteucci, F., Brocato, E., 1990, *ApJ*, **365**, 539.

Pagel, B. E. J., Edmunds. M. G., 1981, *ARAA*, **19**, 77.

Richer, M. G., McCall, M. L., 1995, *ApJ*, **445**, 642.

Zijlstra, A. A., Walsh, J. R., 1996, *A&A*, **312**, L21.

Walsh, J. R., Dudziak, G., Zijlstra, A. A., 1996, in prep.

Albert Zijlstra
e-mail: azijlstr@eso.org

The Distribution of Ionised Gas in Early-Type Galaxies

W.W. ZEILINGER[1], P. AMICO[2], G. BERTIN[3], F. BERTOLA[4], L.M. BUSON[5], I.J. DANZIGER[6, 2], H. DEJONGHE[7], A. PIZZELLA[4], E.M. SADLER[8] R.P. SAGLIA[9] and P.T. DE ZEEUW[10]

[1]Institut für Astronomie, Universität Wien; [2]ESO-Garching; [3]Scuola Normale Superiore, Pisa; [4]Dipartimento di Astronomia, Università di Padova; [5]Osservatorio Astronomico di Capodimonte, Napoli [6]Osservatorio Astronomico, Trieste; [7]Sterrenkundig Observatorium, Universiteit Gent; [8]School of Physics, University of Sydney; [9]Universitäts-Sternwarte München; [10]Sterrewacht Leiden

1. Introduction

The presence of significant amounts of interstellar matter (ISM) in early-type galaxies has been recognised only in recent years (see Macchetto *et al.,* 1996 and references therein). The ISM appears to be more complex than in spiral galaxies. Several components have been identified so far: hot (10^7 K) X-ray gas (typical mass range 10^8–10^{10} $M_\odot$), warm (10^4 K) ionized gas (10^2–10^4 $M_\odot$) and cold (< 100 K) atomic and molecular gas (10^6–10^8 $M_\odot$). The amount of X-ray gas is directly related to the optical luminosity of the galaxy (White & Sarazin, 1991) as expected in a cooling-flow picture *(e.g.* Thomas *et al.,* 1986). The HI content (Knapp *et al.,* 1985), dust content (Forbes, 1991) and CO content (Lees *et al.,* 1991) are found to be unrelated to the stellar luminosity in contrast to what is observed in spiral galaxies. It seems therefore that the hot ISM is a bulge-related phenomenon and the cold component is disk-related, with little interaction between the two. Recent studies revealed that the presence of dust and gas in early-type galaxies is the rule rather than the exception (Bregman *et al.,* 1992).

There are two main sources for the observed non-stellar material: either it is coeval with the stars, resulting from stellar mass loss or it is accreted from outside in a second event in the galaxy history. Faber & Gallagher (1976) investigated how much gas may be produced by stellar evolutionary processes. Assuming a stellar mass-loss rate of 0.015 $M_\odot$/ year, 10^9–10^{10} $M_\odot$ of gas can be accumulated over a Hubble time for a typical elliptical galaxy. In the accretion sce-

TABLE 1: Object list.

Object	RSA Type	RC3 Type	B_T	cz [km/s]	
NGC 484		SA0$^-$	13.1	5200	imaging
NGC 745		S0$^+$pec	14.0	5953	imaging
NGC 1395	E2	E2	10.5	1699	imaging
NGC 1453	E0	E2–3	12.6	3933	imaging & spectroscopy
ESO 118-G34		S0^{0}pec	13.5	1171	imaging
NGC 1947	S0$_3$(0)pec	S0$^-$ pec	11.6	1157	imaging
NGC 2974	E4	E4	11.9	2006	imaging & spectroscopy
NGC 3962	E1	E1	11.6	1818	imaging & spectroscopy
NGC 4636	E0/S0$_1$(6)	E0-1	10.4	927	imaging & spectroscopy
NGC 5846	S0$_1$(0)	E0-1	11.0	1710	imaging & spectroscopy
NGC 6868	E3/S0$_{2/3}$(3)	E2	11.7	2858	imaging & spectroscopy
ESO 234-G21		SA0^{0}pec	13.9	5430	imaging
NGC 7097	E4	E5	12.6	2539	imaging & spectroscopy
NGC 7302	S0$_1$(4)	SA(s)0$^-$	13.2	2586	imaging
IC 1459	E4	E	11.0	1691	imaging

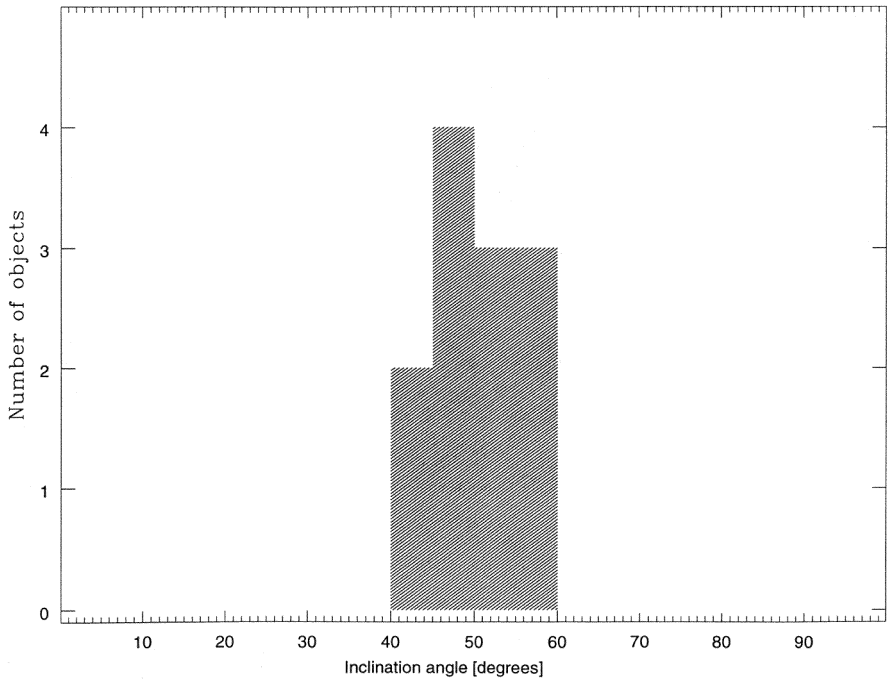

Figure 1: Distribution of inclination angles for the programme galaxies derived gas disk geometry under the assumption of a circular structure.

nario, a typical elliptical galaxy may collect up to $\simeq 10^{10}$ $M_\odot$ of gas over a Hubble time by interaction with its environment (Schweizer, 1983). The conspicuous class of dust-lane ellipticals are explained in this framework. A gaseous disk in an elliptical galaxy which is seen close to edge-on ($i \simeq 80°$) appears as a dust-lane crossing the stellar body (see review by Bertola, 1992) Disks which are not almost edge-on are more difficult to recognise, and can usually be detected only by the presence of emission lines which arise from the ionised gas which is associated with the dust. The key argument in favour for the external origin of the gaseous matter is that in many cases the kinematics of gas and stars are decoupled.

Physical properties of the ISM are expected to hold clues to the formation and subsequent evolution of elliptical galaxies both as dynamical systems and as aggregate of ageing stars. One approach of the ESO Key Programme "A search for dark matter in elliptical galaxies" (Bertin *et al.,* 1989) to trace the radial mass distribution was to study elliptical galaxies with embedded gaseous disks. Observations and modelling are described in a series of three papers (Buson *et al.,* 1993; Zeilinger *et al.,* 1996; Pizzella et *al.,* 1996). A sample of 15 elliptical galaxies with extended emission was selected for this study (Table 1). Narrow-band imaging in the light of the [N II]+Hα lines carried out at the ESO/MPI 2.2-m telescope was used to study the distribution of the ionised matter. A subsample of six objects, which have the most disk-like gas distribution, was selected for long-slit spectroscopy at the ESO 3.6-m and ESO/MPI 2.2-m telescopes in order to map the gas velocity field. The photometric and kinematic results were then used to constrain the intrinsic shape and mass distribution of the host galaxy.

2. Physical Properties of the Ionised Gas

The ionized gas is usually confined to the inner regions of the galaxy extending typically 5–15″ from the nucleus. The distribution of the gas appears to be regular. The isophotal major axes of the stellar and gaseous components are frequently misaligned. The isophotes of the gas disks are found to be significantly flatter then those of the stellar distribution supporting the model of an inclined disk. The surface brightness profiles of the gaseous disks closely follow an $R^{1/4}$ law with an effective radius smaller than the one of the stellar component. This is

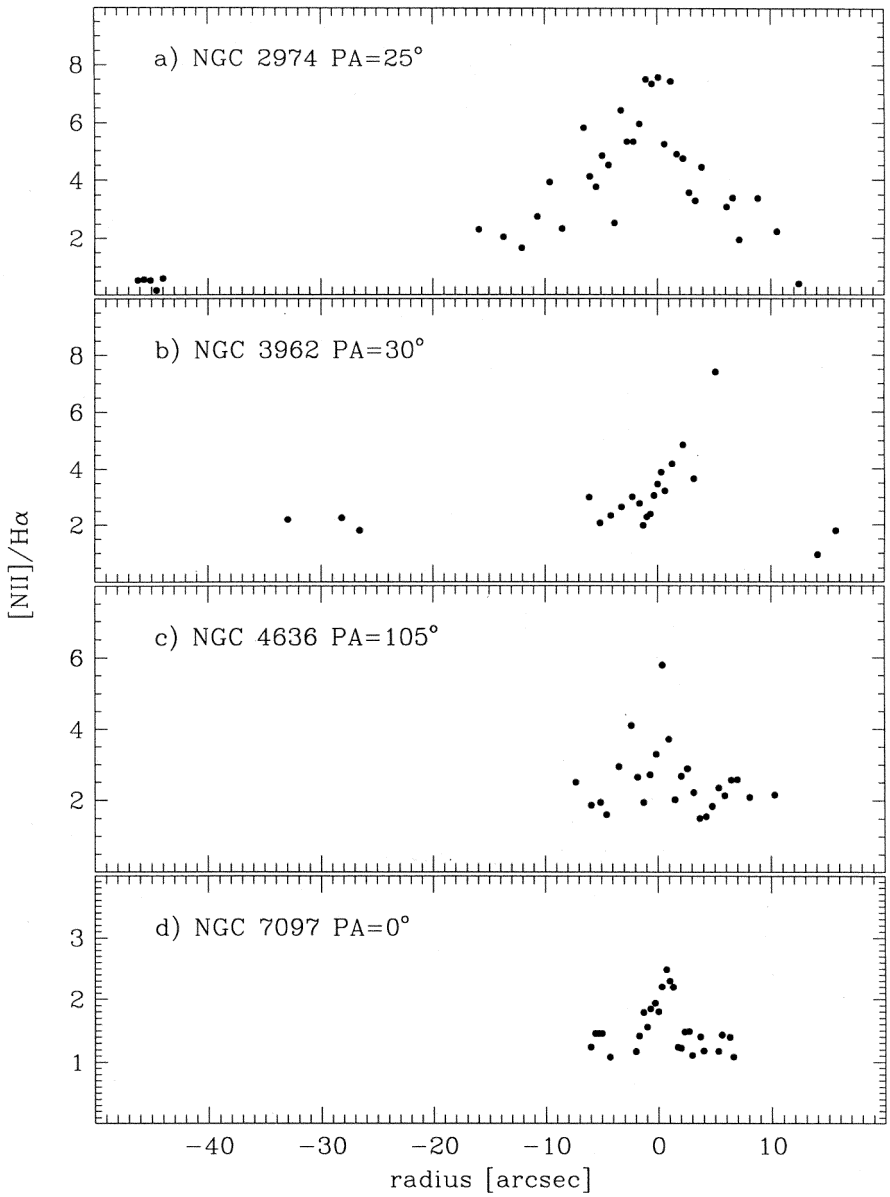

Figure 2: Relative [N II]/Hα flux ratios as function of distance from the galaxy centre for four programme galaxies. ▶

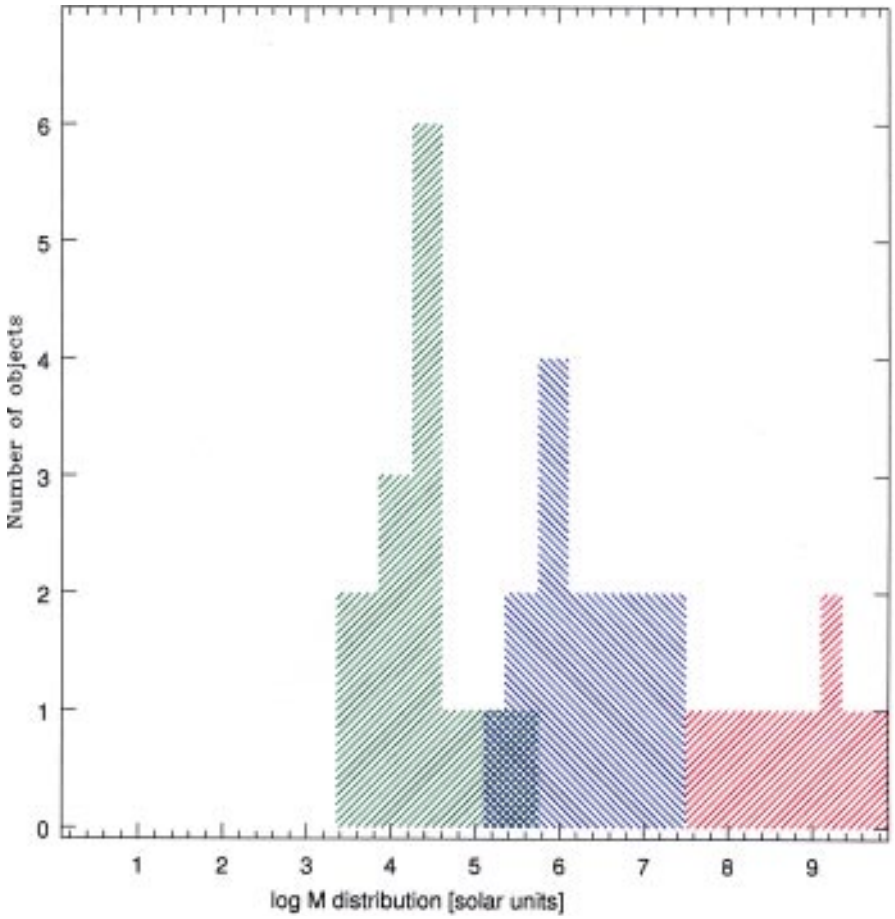

Figure 3: Mass distribution of the three ISM components of the sample galaxies: dust (blue histogram; data from Knapp et al. 1989), ionised gas (green histogram; data from Buson et al. 1993) and X-ray gas (red histogram; data from Roberts et al. 1991).

part of the galaxy are interpreted as high-velocity dispersions indicating a dynamically rather hot gas component. The kinematic data in the central parts of the galaxy (typically R < 4″) are certainly affected by seeing. The lines are blurred and consequently velocity gradients are lowered and lines become broadened. Simulations showed that seeing effects may produce an artificial increase of the velocity dispersion to a maximum of 150 km/s. The observed peak velocity dispersions are however in the range of 200–250 km/s. This could be evidence for a pressure-supported gas in central regions of the galaxy *(e.g.* Bertola *et al.,* 1995).

The spectra of all the sample galaxies are characterised by LINER-type emission indicating nuclear activity as described by Demoulin-Ulrich *et al.,* (1984). The typical [N II]/Hα ratios found are $\geq$ 2 in the central parts of the galaxy (Fig. 2). Hot stars can therefore be ruled out as the only sources of ionisation. A similar conclusion was reached by Phillips *et al.* (1986) for "normal" early-type galaxies. Comparing the radio continuum emission of the programme galaxies with a complete sample, it turns out that galaxies with ionised gas disks have radio powers typically 10–15 times higher then "normal" ellipticals. This would suggest that an active nucleus contributes to the ionisation of the gas disk as is also the case for more powerful FR II radio galaxies (Baum & Heckman, 1989)

in contrast to the distribution of neutral hydrogen in spiral galaxies, where the density profile of the gaseous disks obeys an exponential law with a scale length usually larger than that of the stellar disk (see Wevers, 1984, Kennicutt, 1989). The distribution of inclinations of the sample was derived assuming that the disks are fundamentally flat structures of circular shape. The inclinations range between 45° to 60° (Fig. 1). The lack of face-on disks ($i \simeq 0°$) is due to the fact that the disk is a low-surface-brightness structure and therefore can hardly be seen against the bright background of the galaxy. On the contrary, galaxies with edge-on disks ($i > 75°$) will appear as a dust lane due to the absorbing matter associated with the gas.

The observed gas kinematics is found to be consistent with the picture of the ionised gas being distributed in regular disk-like structures. The rotation pattern follows closely the geometry of the line-emitting region. The presence of large emission-line widths in the central

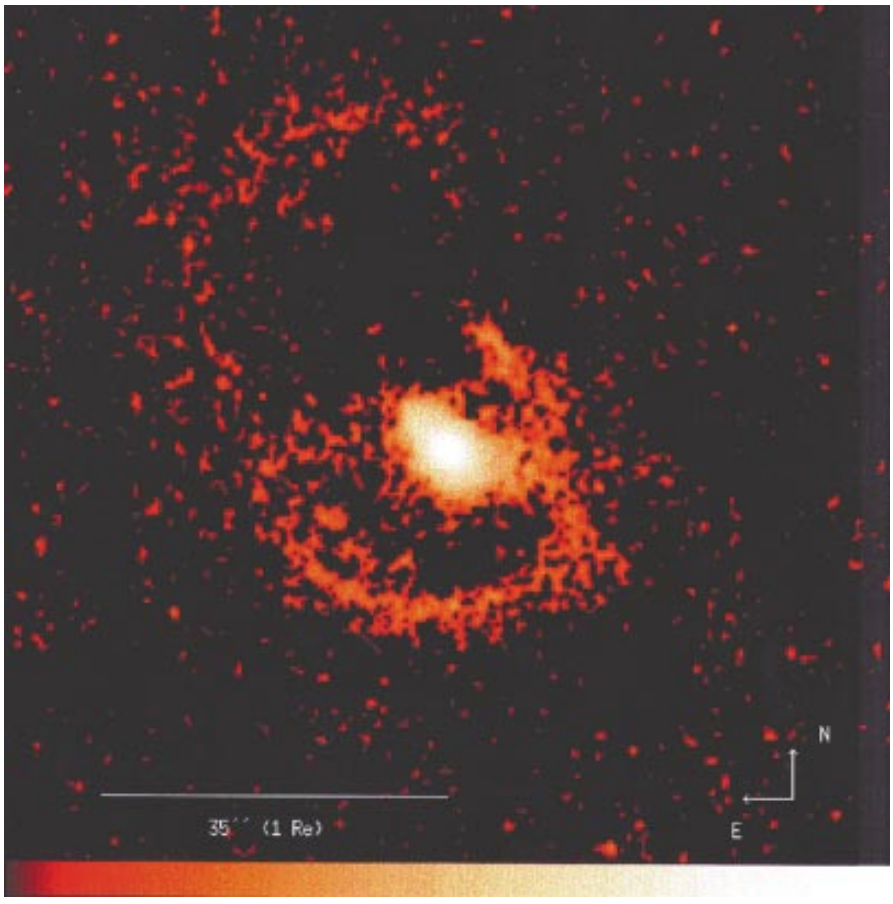

Figure 4: Narrow-band image of NGC 3962 in the light of the [N II]+Hα emission lines obtained at the ESO/MPI 2.2-m telescope with a typical seeing of ≃ 1.1″. The image reveals two distinct ionized gas components: an inner disk-like structure and an outer arc-like structure.

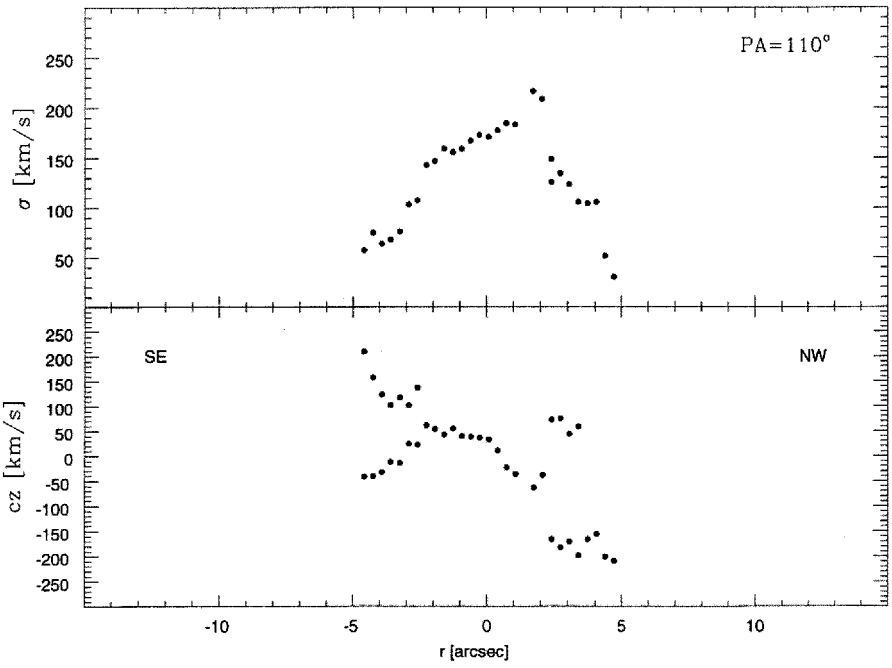

Figure 5: Ionised gas kinematics of NGC 6868 derived from the [N II] A 6583.4 Å line. The spectrum was obtained at the ESO/MPI 2.2-m telescope equipped with EFOSC2. The typical seeing was ≃ 1″ during the exposure. The lower panel displays the radial velocity curve. In the upper panel the velocity dispersion profile is shown.

counter-rotating gas components were discovered (Fig. 5).

3. Gaseous Disks as Probe for the Galactic Potential

The programme galaxies for the modelling were selected as the cases where we established the presence of a regular disk, settled in the potential of the host galaxy (Christodoulou *et al.,* 1992; Katz & Rix, 1992). The gas should then occupy the simple closed orbits of the potential. Earlier work used circular orbits in spherical potentials to model the observed gas kinematics (Caldwell *et al.,* 1986 in the case of NGC 7097). Bertola *et al.,* (1991) used triaxial mass models with a separable potential to model the observed gas kinematics of NGC 5077. These models incorporate the proper shape of the galaxy and allow an exact analytic description of the velocity field, but correspond to density profiles with finite density cores. As a result, the elliptic closed orbits become very elongated in the central region and are unlikely to give the correct description of the gas motions there. In the

The mass distributions of the different phases of the ISM are displayed in Figure 3. The median mass of the X-ray gas is $\simeq 1.5 \times 10^9$ $M_\odot$. A median dust mass of 8×10^5 $M_\odot$ was derived using IRAS measurements as indicator for the cold ISM component. If the dust/gas ratio of the Galaxy applies also to the sample galaxies the median H I mass would be of the order 8×10^7 $M_\odot$. The median mass of the ionised gas is only 6×10^4 $M_\odot$ which, however, would be about 10–100 times higher than in "normal" early-type galaxies of similar optical luminosity. The ionised gas is probably closely related to the cold (atomic and molecular) component of the ISM as also suggested by Macchetto & Sparks (1992). Under this assumption the ionised gas would contribute significantly less than 1% to the total mass of the cold component. The kinematics of the ionized gas would consequently be dominated by the underlying cold gas disk and the amount of ionized gas which is seen will depend on the number of ionised photons available rather than on the amount of gas present. This would also explain why the gas velocity field is regular despite a morphology which in some cases appears disturbed.

The analysis of the observational material revealed a number of peculiarities strongly supporting the view that significant amounts of gas result from external accretion. NGC 3962 exhibits two distinct gas structures: an elongated central disk-like component and an arm-like structure extending from the major axis of the inner gas disk (Fig. 4). The line of nodes of the two components are significantly misaligned. In NGC 6868 two

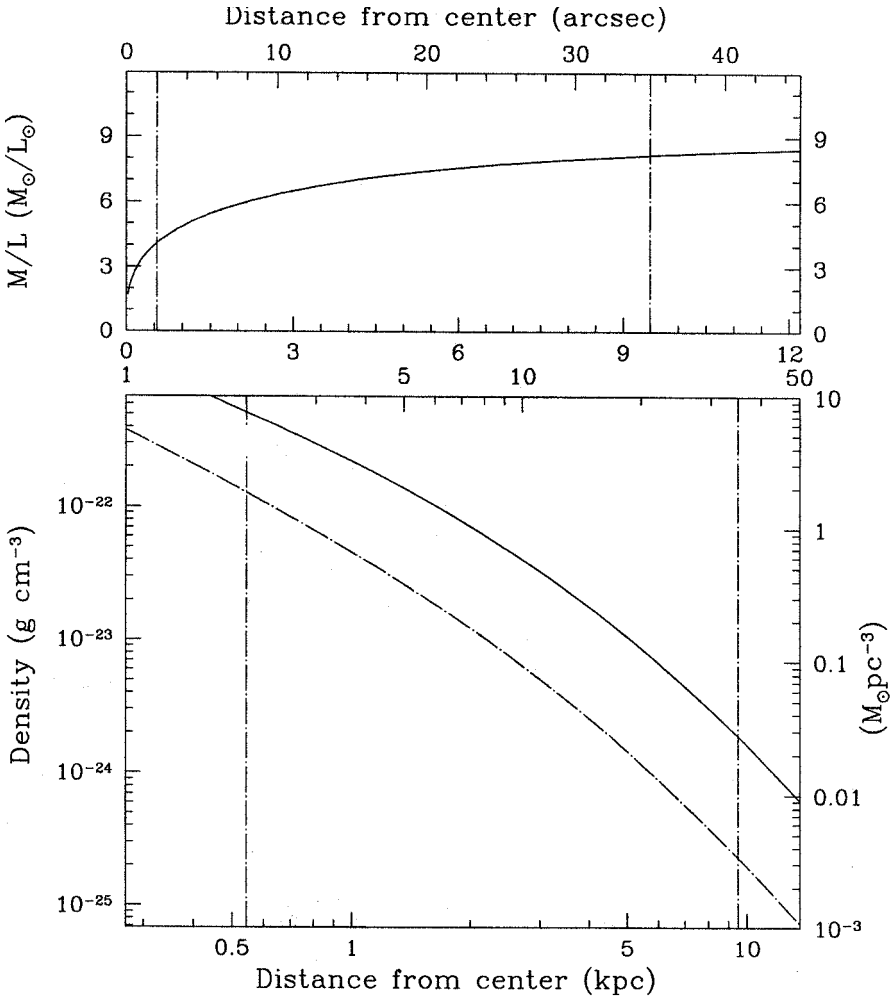

Figure 6: NGC 5077: lower panel: Mass (full line) and light (long-dashed line) density profiles. upper panel: local M/L_B ratio as a function of radius.
The vertical lines define the regions where the modelling results are valid. The inner limit is defined by the seeing while the outer limit is given by the last observed kinematical data point. H_0 is 50 km/s/Mpc.

present study, a family of non-rotating triaxial mass models was used with a central density cusp as observed in the centres of many ellipticals (Crane *et al.,* 1993). These models allow for variations of ellipticity and position angle of major-axis isophotes. They are described in detail by de Zeeuw & Carollo (1996).

Out of the original sample only three galaxies (NGC 1453, NGC 2974 and NGC 7097) turned out to be suitable for modelling. In the remaining objects either presence of several gas components or non-regularities in the velocity field preclude modelling with the gas settled on simple closed orbits. The data of NGC 5077 were also modelled to be compared with the results of Bertola *et al.* (1991). The new model is found to be in reasonable agreement, but better constrained due to the more restrictive geometry (allowing for isophotal twisting). The modelling yielded for NGC 2974 and NGC 7097 that the gas moves on a plane perpendicular to the intrinsic minor axis while in NGC 1453 and NGC 5077 the gas occupies a plane perpendicular to the intrinsic major axis of the galaxy. This would also support the view of the external origin of the gaseous matter.

The resulting mass and light density profiles together with the radial trend of the local M/L_B ratio of NGC 5077 is displayed in Figure 6 as an example for the whole sample. The derived M/L profiles do not show significant radial variations. The M/L ratio seems to be higher for objects of higher optical luminosity. A mean value of $M/L \simeq 5\ M_\odot/L_\odot$ within 1 R_e was derived for the sample. This suggests that the central regions of elliptical galaxies are essentially dominated by luminous matter while dark matter becomes dynamically important only in the range of 2–3 R_e; in this region, however, one has to use the information provided by the stellar kinematics *(e.g.* Saglia *et al.,* 1993; Bertin *et al.,* 1994; Carollo *et al.,* 1995) or resort to other tracers of the gravitational field (Bertola *et al.,* 1993). The use of X-ray data, which extend out to typically $\simeq 7\ R_e$ is not straightforward *(c.f.* Bertin *et al.,* 1993), although a recent combination of ASCA and ROSAT data allowed more precise constraints on the mass distributions for NGC 720 and NGC 1332 (Buote & Canizares, 1997).

The ionised gas proves to be a good tracer of the potential of the host galaxy when compared with stellar kinematical results as in the case of NGC 2974 (Cinzano & van der Marel, 1994).

Acknowledgements

A.P. acknowledges support from a *Acciaierie Beltrame* grant. R.P.S. acknowledges the financial support by the Deutsche Forschungsgemeinschaft under SFB 375. W.W.Z. acknowledges the support of the Hochschuljubiläumstiftung der Stadt Wien (project H-112/95).

References

Baum, S.A. & Heckman, T., 1989, *Astrophys. J.,* **336**, 69.
Bertin, B., Bertola, F., Buson, L.M., Danziger, I.J., Dejonghe, H., Sadler, E.M., Saglia, R.P., Vietri, M., de Zeeuw, P.T. & Zeilinger, W.W.:, 1989, *The Messenger,* **56**,19.
Bertin, G., Bertola, F., Buson, L.M., Danziger, I.J., Dejonghe, H., Sadler, E.M., Saglia, R.P., de Zeeuw, P.T. & Zeilinger, W.W., 1994, *Astron. Astroph., **292,*** 381.
Bertin, G., Pignatelli, E. & Saglia, R.P., 1993, *Astron. Astroph.,* **271**, 381.
Bertola, F. 1992 in *"Morphological and Physical Classification of Galaxies"* ed. Longo, G. et *al., p.* 115.
Bertola, F., Bettoni, D., Danziger, I.J., Sadler, E.M., Sparke, L.S. & de Zeeuw, 1991, *Astrophys. J.,* **373**, 369.
Bertola, F., Pizzella, A., Persic, M. & Salucci, P., 1993, *Astrophys. J.,* **416**, L45.
Bertola, F., Cinzano, P., Corsini, E.M., Rix, H.W. & Zeilinger, W.W., 1995, *Astrophys. J.,* **448**, L13.
Bregman, J.N., Hogg, D.E. & Roberts, M.S., 1992, *Astrophys. J.,* **387**, 484.
Buote, D.A. & Canizares, C.R., 1997, *Astrophys. J.,* in press.
Buson, L.M., Sadler, E.M., Zeilinger, W.W., Bertin, G., Bertola, F., Danziger, I.J., Dejonghe, H., Saglia, R.P. & de Zeeuw, P.T., 1993, *Astron. Astroph.,* **280**, 409.
Caldwell, N., Kirshner, R.P. & Richstone, D.O., 1986, *Astrophys. J.,* **305**, 136.
Carollo, C.M., de Zeeuw, P.T., van der Marel, R.P., Danziger, I.J. & Qian, E.E., 1995, *Astrophys. J.,* **441**, L25.
Cinzano, P. & van der Marel, R.P., 1994, *Mon. Not. R. astr. Soc.,* **270**, 325.
Crane, P. *et al.* 1993, *Astron. J.,* **106**, 1371.
Christodoulou, D.M., Katz, N., Rix, H.W. & Habe, A., 1992, *Astrophys. J.,* **395**, 113.
Demoulin-Ulrich, M.H., Butcher, H.R. & Boksenberg, A., 1984, *Astrophys. J.,* **285**, 527.
Faber, S.M. & Gallagher, J.S, 1976, *Astrophys. J.,* **204**, 365.
Forbes, D.A., 1991, *Mon. Not. R. astr. Soc.,* **249**, 779.
Katz, N. & Rix, H.W., 1992, *Astrophys. J.,* **389**, L55.
Kennicutt, R.C., 1989, *Astrophys. J.,* **344**, 685.
Isnapp, G.R., Turner, E.C. & Cunniffe, P.E., 1985, *Astron. J., **90,*** 454.
Knapp, G.R., Guhathakurta, P., Kim, D.-W. & Jura, M., 1989, *Astrophys. J. Suppl.,* **70**, 387.
Lees, J.F., Knapp, G.R., Rupen, M.P. & Phillips, T.G., 1991, *Astrophys. J.,* **379**, 177.
Macchetto, F. & Sparks, W.B., 1992 in *"Morphological and Physical Classification of Galaxies"* ed. Longo, G. *et al., p.* 191.
Macchetto, F., Pastoriza, M., Caon, N., Sparks, W.B., Giavalisco, M., Bender, R. & Capaccioli, M., 1996 *Astron. Astroph.,* in press.
Phillips, M.M., Jenkins, C.R., Dopita, M.A., Sadler, E.M. & Binette, L., 1986, *Astron. J., **91,*** 1062.
Pizzella, A., Amico, P., Bertola, F., Buson, L.M., Danziger, I.J., Dejonghe, H., Sadler, E.M., Saglia, R.P, de Zeeuw, P.T. & Zeilinger, W.W., 1996 *Astron. Astroph.,* submitted.
Roberts, M.S., Hogg, D.E., Bregman, J.N., Forman, W.R. & Jones, C., 1991, *Astrophys. J. Suppl.,* **75**, 751.
Saglia, R.P., Bertin, B., Bertola, F., Danziger, I.J., Dejonghe, H., Sadler, E.M., Stiavelli, M., de Zeeuw, P.T. & Zeilinger, W.W., 1993, *Astrophys. J., **403,*** 567.
Schweizer, F., 1983, IAU Symp. **100**, p. 319.
Thomas, P.A., Fabian, A.C., Arnaud, K.A., Forman, W. & Jones ,C., 1986, *Mon. Not. R. astr. ,Soc.,* **222**, 655.
Wevers, B.M.R.H. 1984, Ph.D. diss., University of Groningen.
White, III, S. & Sarazin, C.L., 1991, *Astrophys. J.,* **367**, 476.
de Zeeuw, P.T. & Carollo, C.M., 1996, *Mon. Not. R. astr. Soc.,* in press.
Zeilinger, W.W., Pizzella, A., Amico, P., Bertin, G., Bertola, F., Buson, L.M., Danziger, I.J., Dejonghe, H., Sadler, E.M., Saglia, R.P. & de Zeeuw, P.T., 1996, *Astron. Astroph., in* press .

Werner Zeilinger
e-mail: wzeil@doradus.ast.univie.ac.at

The Challenging Type Ia SN 1991bg in the Virgo Galaxy NGC 4374

M. TURATTO [1, 2], S. BENETTI [1], E. CAPPELLARO [2], I.J. DANZIGER [1, 3], P.A. MAZZALI [3]

[1]European Southern Observatory;
[2]Osservatorio Astronomico di Padova; [3]Osservatorio Astronomico di Trieste, Italy

The long-standing effort in studying type Ia Supernovae (SN Ia) has been motivated in part by their use as distance indicators. Several publications have recently been devoted to the absolute calibration of SN Ia up to the distance of the Virgo cluster using the Cepheids discovered by HST in the SN parent galaxies. It is now commonly believed that the average absolute magnitude of SN Ia at maximum is close to $M_B = -19.5$, while the average